

# Gaussian boson sampling and multi-particle event optimization by machine learning in the quantum phase space

Claudio Conti\*

*Department of Physics, University Sapienza, P.le Aldo Moro 5, 00185 Rome, Italy  
Institute for Complex Systems, National Research Council (ISC-NR), Via dei Taurini 19, 00185 Rome, Italy and  
Research Center Enrico Fermi, Via Panisperna 89a, 00184 Rome (Italy) †*

(Dated: February 25, 2021)

We use neural networks to represent the characteristic function of many-body Gaussian states in the quantum phase space. By a pullback mechanism, we model transformations due to unitary operators as linear layers that can be cascaded to simulate complex multi-particle processes. We use the layered neural networks for non-classical light propagation in random interferometers, and compute boson pattern probabilities by automatic differentiation. We also demonstrate that multi-particle events in Gaussian boson sampling can be optimized by a proper design and training of the neural network weights. The results are potentially useful to the creation of new sources and complex circuits for quantum technologies.

The development of new models and tools for machine learning (ML) is surprisingly affecting the study of many-body quantum systems and quantum optics. Neural networks (NN) enable representations of high-dimensional systems and furnish a universal ansatz for many purposes, like finding the ground state of many-body Hamiltonians [1], including dissipative systems [2, 3].

Unsupervised and supervised learning endow new designs for quantum circuits [4], metrology and cryptography [5, 6], multilevel gates [7], and Bell tests [8]. NN are also triggering new fundamental investigations in quantum neuromorphic and wave computing [9–14], quantum thermodynamics [15], and topological photonics [16].

The impact of ML in quantum optics and many-body physics is related to the versatile representation that the NN models furnish for functions of an arbitrary number of variables. Also, the powerful application programming interfaces (APIs), as `TensorFlow`, enable many new features and tools to compute and design many-body Hamiltonians or large-scale quantum gates [17].

Here we show that NN models are also useful when considering representations in the phase space, as the characteristic functions  $\chi$  or the Q-representation [18]. Unitary operators, as squeezers or displacers, act on the phase-space as variable transformations that correspond to layers in the NN model. Hence, a multilayer NN may encode phase-space representations of complex many-body states. This encoding has two main advantages: on the one hand, one can quickly build complex quantum states by combining NN layers; on the other hand, one can use the automatic graph building and API differentiation technology to compute observables. Also, graphical and tensor processing units (GPU and TPU) may speed up the computation.

In the following, we show how to compute the probability of multi-particle patterns when Gaussian states propagate in a system made of squeezers and interferometers. This problem corresponds to the renowned Gaussian Boson sampling [19, 20], which recently demonstrated the

quantum advantage at an impressive scale [21], following earlier realizations [22–27] of the original proposal by Aharonson and Arkhipov [28]. The theory of Gaussian Boson sampling (GBS) heavily relies on phase-space methods [29], making it an exciting NN test-bed.

A notable outcome of adopting NN models in the phase space is the possibility of training multi-particle statistics and other features as the degree of entanglement. Indeed, most of the reported investigations in quantum ML, focus either on using NN models as a variational ansatz or tailoring the input/output response of a quantum gate. On the contrary, ML in the phase space permits optimizing many-particle features, for example, to increase the probability of multi-photon events. NN may open new strategies to generate non-classical light or enhance the probability of observing large-scale entanglement with relevance in many applications. Here, we derive the NN representing the characteristic function of the Gaussian boson sampling setup. Proper NN training increases the photon-pair probability by orders of magnitude.

In the phase space, we represent a  $n$ -body state by complex characteristic function  $\chi(\mathbf{x}) = \chi_R(\mathbf{x}) + \imath\chi_I(\mathbf{x})$  of a real vector  $\mathbf{x}$  [18, 30].  $\mathbf{x}$  has dimension  $1 \times N$  with  $N = 2n$ . For Gaussian states [31]

$$\chi(\mathbf{x}) = e^{-\frac{1}{4}\mathbf{x}\mathbf{g}\mathbf{x}^\top + \imath\mathbf{x}\mathbf{d}}. \quad (1)$$

with  $\mathbf{g}$  the real covariance  $N \times N$  matrix, and  $\mathbf{d}$  the real displacement  $N \times 1$  vector. In our notation, we omit the symbols of the dot product such that  $\mathbf{x}\mathbf{d}$  and  $\mathbf{x}\mathbf{g}\mathbf{x}^\top$  are scalars. One has ( $j, k = 0, 1, 2, \dots, N - 1$ )

$$\langle \hat{R}_j \rangle = d_j = \left. \frac{\partial \chi}{\partial x_j} \right|_{\mathbf{x}=0}, \quad (2)$$

and

$$g_{jk} = 2\langle (\hat{R}_j - d_j)(\hat{R}_k - d_k) \rangle - \imath J_{jk}, \quad (3)$$

being  $\mathbf{J} = \bigoplus_{j=0}^{n-1} \mathbf{J}_1$ ,  $\mathbf{J}_1 = \begin{pmatrix} 0 & 1 \\ -1 & 0 \end{pmatrix}$  [31]. In Eq. (2), the canonical variables,  $\hat{q}_j = \hat{R}_{2j}$  and  $\hat{p}_j = \hat{R}_{2j+1}$ , with  $j =$

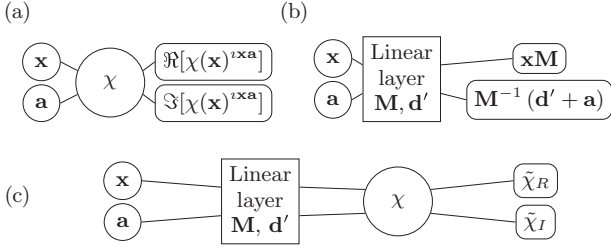


FIG. 1. (a) A neural network model for the characteristic function. Two inputs, a data vector  $\mathbf{x}$  with shape  $1 \times N$  and a bias vector  $\mathbf{a}$  with shape  $N \times 1$  seed the model that compute  $\chi$  and returns the real and imaginary parts of  $\chi(\mathbf{x})e^{i\mathbf{x}\mathbf{a}}$ . (b) A layer representing a linear transformation of the state by a unitary operator represented by a symplectic  $N \times N$  matrix  $\mathbf{M}$  and a displacement  $N \times 1$  vector  $\mathbf{d}'$ . With such a definition layers can be cascaded, and one can represent single mode squeezers, interferometers, and other unitary operators. (c) A model representing a state with characteristic function  $\chi$ , subject to a unitary transformation. This is a pullback of a linear transform from the original state, which produces a new state with characteristic function  $\tilde{\chi}$  [see Eq. (4)].

$0, 1, \dots, n-1$ , are organized in the  $N \times 1$  operator array  $\hat{\mathbf{R}}$ . As shown in Fig. 1a, the characteristic function is a NN layer with two real outputs  $\chi_R$  and  $\chi_I$ . The  $\chi$  layer has two inputs:  $\mathbf{x}$ , and a auxiliary bias  $N \times 1$  vector  $\mathbf{a}$ , for later convenience.

The vacuum state is a Gaussian state with  $\mathbf{g} = \mathbf{1}$  and  $\mathbf{d} = \mathbf{0}$ . From the vacuum, one can generate specific states by unitary operators, as displacement or squeezing operators. These transform the canonical variables as  $\hat{\mathbf{R}} = \mathbf{M}\hat{\mathbf{R}} + \mathbf{d}'$ , where the symplectic matrix  $\mathbf{M}$  and the vector  $\mathbf{d}'$  depend on the specific operator (detailed, e.g., in [31]). The characteristic function changes as

$$\tilde{\chi}(\mathbf{x}) = \chi(\mathbf{x}\mathbf{M})e^{i\mathbf{x}\mathbf{d}'+i\mathbf{x}\mathbf{a}} = \chi(\mathbf{x}\mathbf{M})e^{i(\mathbf{x}\mathbf{M})\mathbf{M}^{-1}(\mathbf{d}'+\mathbf{a})} \quad (4)$$

We represent the linear transformation as a NN layer with two inputs  $\mathbf{x}$  and  $\mathbf{a}$  and two outputs  $\mathbf{x}\mathbf{M}$  and  $\mathbf{M}^{-1}(\mathbf{d}'+\mathbf{a})$  (Fig. 1b). By this definition, Eq. (4) is as a two-layer NN. Figure 1c shows  $\tilde{\chi}$  as the ‘‘pullback’’ of the linear layer from the  $\chi$  layer. The two layers form a NN that can be implemented with common APIs. [32].

Given the vacuum state with characteristic function  $\chi$ , one can build the NN model of an arbitrary state by multiple pullbacks. Indeed, we defined the linear layers in a way that they can be cascaded. Figure 2a shows a  $n$ -mode squeezed vacuum as a multiple pullback of single mode squeezers, each acting on a different mode.

Observable can be computed as derivatives of the NN model. For example, the mean photon number per mode is related to the derivatives of the characteristic function. In our notation, the mean photon number for mode  $j$ , is

$$\langle \hat{n}_j \rangle = -\frac{1}{2} (\nabla_j^2 + 1) \chi \Big|_{\mathbf{x}=\mathbf{0}} \quad (5)$$

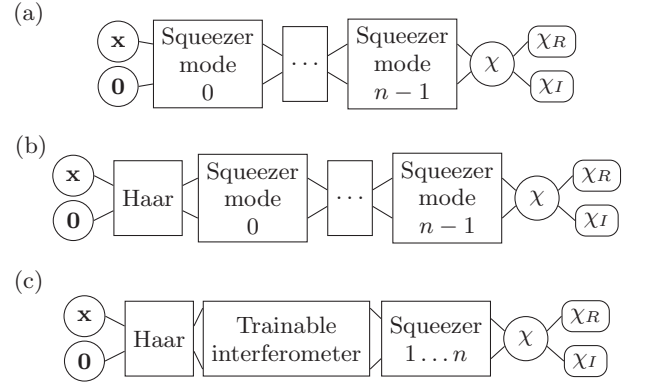


FIG. 2. (a) A multiple pullback that represents a many-body squeezed vacuum, obtained by a vacuum state  $\chi$  by cascading  $n$  identical single mode squeezers. The order of the squeezers is not relevant as they act of different modes.  $\chi_R$  and  $\chi_I$  are the real and imaginary part of the resulting characteristic function. (b) GBS setup, a  $n$ -body squeezed vacuum enters an Haar interferometer. Note that the order of the operators, from the vacuum to the interferometer goes from right to left. (c) GBS setup including a trainable random interferometer before entering the Haar interferometer. The multiple squeezers are represented as a single block. The trainable interferometer can be realized by light modulators to optimize the probability of pair generation.

being  $\nabla_j^2 = \partial_{q_j}^2 + \partial_{p_j}^2$  and  $q_j = x_{2j}$  and  $p_j = x_{2j+1}$ . The differential photon number of modes  $j$  and  $k$  is

$$\langle (\hat{n}_j - \hat{n}_k)^2 \rangle = \left[ \frac{1}{4} (\nabla_j^2 - \nabla_k^2)^2 - \frac{1}{2} \right] \chi \Big|_{\mathbf{x}=\mathbf{0}}. \quad (6)$$

Derivatives of the NN model can be computed by the automatic differentiation packages.

In the GBS protocol, one considers a many-body squeezed vacuum state propagating in an Haar interferometer, which distributes the photons in the output modes. For modelling GBS, we hence need squeezing layers and a layer representing transmission through random interferometers. The squeezing layers are realized by a proper design of the corresponding symplectic matrices  $\mathbf{M}$  with  $\mathbf{d} = \mathbf{0}$ . We implement the Haar matrix operator by QuTiP software [33]. Figure 2b shows a graphical representation of the GBS NN model [19].

Boson sampling corresponds to computing the probability  $\text{Pr}(\bar{\mathbf{n}})$  of finding  $\bar{n}_0$  photons in mode 0,  $\bar{n}_1$  photons in mode 1, and so forth, where  $\bar{\mathbf{n}} = (\bar{n}_0, \bar{n}_1, \dots, \bar{n}_{n-1})$  is a given photon pattern. Letting  $\hat{\rho}$  the density matrix, one has  $\text{Pr}(\bar{\mathbf{n}}) = \text{Tr}[\hat{\rho}|\bar{\mathbf{n}}\rangle\langle\bar{\mathbf{n}}|]$ , with  $|\bar{\mathbf{n}}\rangle\langle\bar{\mathbf{n}}| = \otimes_{j=0}^{n-1} |\bar{n}_j\rangle\langle\bar{n}_j|$ . Correspondingly [29],

$$\text{Pr}(\bar{\mathbf{n}}) = \frac{1}{\bar{\mathbf{n}}!} \prod_{j=0}^{n-1} \left( \frac{\partial^2}{\partial \alpha_j \partial \alpha_j^*} \right)^{\bar{n}_j} e^{\sum_j |\alpha_j|^2} Q_\rho(\boldsymbol{\alpha}, \boldsymbol{\alpha}^*) \Big|_{\boldsymbol{\alpha}=\mathbf{0}} \quad (7)$$

where  $\bar{\mathbf{n}}! = \bar{n}_0! \bar{n}_1! \dots \bar{n}_{n-1}!$  and  $Q_\rho = \pi^n \langle \boldsymbol{\alpha} | \rho | \boldsymbol{\alpha} \rangle$  is the Q-representation of the density matrix [18, 30] with  $\boldsymbol{\alpha} =$

$(\alpha_0, \alpha_1, \dots, \alpha_{n-1})$  complex displacements.

We introduce the  $N \times 1$  real vector  $\mathbf{k}$  as  $k_{2j} = (\alpha_j + \alpha_j^*)/\sqrt{2}$ ,  $k_{2j+1} = -(\alpha_j - \alpha_j^*)/\sqrt{2}i$  and we have

$$\Pr(\bar{\mathbf{n}}) = \frac{1}{\bar{\mathbf{n}}!2^{\bar{n}_T}} \left( \prod_j \tilde{\nabla}_j^{2\bar{n}_j} \right) e^{\frac{\mathbf{k}^2}{2}} Q_\rho(\mathbf{k}) \Big|_{\mathbf{k}=0} \quad (8)$$

with  $\tilde{\nabla}_j^2 = \partial^2/\partial k_{2j} + \partial^2/\partial k_{2j+1}$  and  $\bar{n}_T = \sum_{j=0}^{n-1} \bar{n}_j$ .  $Q_\rho$  in Eq. (8) can be evaluated explicitly as a multidimensional Gaussian integral:

$$\Pr(\bar{\mathbf{n}}) = \frac{1}{\bar{\mathbf{n}}!2^{\bar{n}_T}} \left( \prod_j \tilde{\nabla}_j^{2\bar{n}_j} \right) \mathcal{Q}(\mathbf{k}) \Big|_{\mathbf{k}=0} \quad (9)$$

with  $(p, q = 0, 1, \dots, N-1)$

$$\mathcal{Q}(\mathbf{k}) = \frac{1}{\sqrt{2^n \det A}} e^{\frac{1}{2}\mathbf{k}^2} e^{-\frac{1}{2}\sum_{pq} A_{pq}^{-1}(k_p - d_q)(k_p - d_q)} \quad (10)$$

being  $A_{pq} = \frac{1}{2}(g_{pq} + \delta_{pq})$ . Eq. (9) and (10) can be implemented as further layers of the NN, and the probability of a given pattern computed by running the model.

Figure 3a shows an example of the pattern probability distribution with  $n = 6$ , obtained by using the NN model in Fig. 2b with squeezing parameters  $r_j = 0.88$  and  $\phi_j = \pi/4$ , such that all the single mode squeezers are identical, each with mean photon number  $\sinh(r_j)^2 \simeq 1$ . As in [19], we consider patterns with  $\langle \hat{n}_j \rangle = \{0, 1\}$ .

Our interest is understanding if we can train the model to maximize the generation of specific patterns, e.g., a photon pair in modes 0 and 1. Using complex media to tailor the response of linear systems is a well renowned technique as, for example, to synthesize specific gates [34, 35] or taming entanglement [36]. Here, we use the NN model in the phase space to optimize multi-particle events by using GBS.

One could use the squeezing parameters in the model in Fig. 2b as training parameters. However, the degree of squeezing affects the number of particles per mode, and we want to alter the statistical properties of states without changing the average number of particles. We hence consider a GBS setup with an additional trainable interferometer as in Fig. 2c, which is typically realized by amplitude or phase modulators.

In Fig. 2c,  $n$  squeezed vacuum modes impinge on a trainable interferometer and then travel through a Haar interferometer. Instead of two distinct interferometers, one could use a single device (i.e., combine the Haar interferometer with the trainable interferometer), but we prefer to distinguish the trainable part from the mode-mixing Haar unitary operator.

Given  $n$  modes, our goal is to maximize the probability of patterns that contains a pair of photons in the mode 0 or 1. For example, for  $n = 6$ , this means maximizing

the probability of  $\bar{\mathbf{n}} = (1, 1, 0, 0, 0, 0)$  with respect to  $\bar{\mathbf{n}} = (1, 0, 0, 1, 0, 0)$ . We use as loss function

$$\mathcal{L} = e^{\langle (\hat{n}_0 - \hat{n}_1)^2 \rangle} \quad (11)$$

which is minimal when the expected differential number of photons in mode 0 and mode 1 vanishes. This is the case when the state has a particle pair in mode 0 and mode 1. More sophisticated loss functions can be considered, but we use Eq. (11) for the sake of simplicity and to limit the computational time.

We stress the difference in using other cost functions, which involve the expected number of photons per mode as, e.g.,  $e^{\langle (\hat{n}_0) - \langle \hat{n}_1 \rangle \rangle^2}$ . As the linear interferometer does not affect the average number of photons (which are mixed by the Haar interferometer), training would not be effective. On the contrary, Eq. (11) contains  $\langle \hat{n}_0 \hat{n}_1 \rangle$ , which is maximal with a photon pair in modes 0 and 1.

Fig. 3a shows the computed probabilities of pairs for the model in Fig. 2c, with a random instance of the Haar and the linear interferometers. Training strongly alters this statistical distribution, as shown in Fig. 3b. Fig. 3c shows the trend during the training epochs of  $\langle (\hat{n}_0^2 - \hat{n}_1^2) \rangle$ , which goes to zero while the mean photon numbers  $\langle \hat{n}_0 \rangle$  and  $\langle \hat{n}_1 \rangle$  remain unaltered.

Training also maximizes higher photon events, as in the pattern  $\bar{\mathbf{n}} = (1, 1, 1, 1, 0, 0)$  with 4 photons and  $n = 6$ . Fig. 4a shows the pattern probability with 4 photons. After training with the loss function in Eq. (11),  $\Pr(\bar{\mathbf{n}})$  substantially increases for the patterns with four photons containing 1 pair in modes 0 and 1 (Fig. 4b).

*Discussion* — We have shown that a many-body characteristic function may be reformulated as a layered neural network. This model enables to build complex states for various applications, as gate design or boson sampling, and computing observables as derivatives.

A common argument in criticizing quantum neural networks is that the linear quantum mechanics does not match with the nonlinearity-eager NN models. However, if we formulate quantum mechanics in the phase space, nonlinearity arises in the characteristic function (or other representation), as shown here in the simplest case of Gaussian states. Hence the resulting model is universal and may be trained for different purposes.

Phase space models allow naturally in dealing with non-classical states, as in the presence of squeezing and entanglement. An ML approach in the phase-space, with states identified by highly nonlinear (non-polynomial) functions of many variables, and observables by their derivatives, opens many opportunities. For example, the optimization of multi-particle events in the phase space can be extended to fermionic fields. On the other hand, computing boson patterns probabilities by NN APIs is not expected to be competitive with highly optimized algorithms running on large-scale clusters [37, 38]. Still, it appears to be a versatile and straightforward approach.

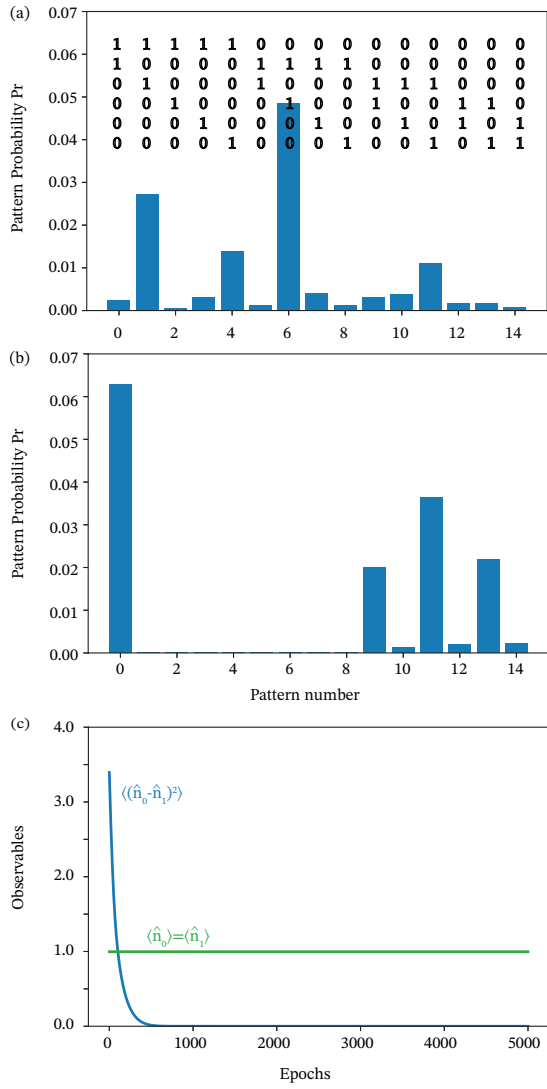


FIG. 3. (a) Probability distribution of patterns with two photons for  $n = 6$  in the model in Fig. 2c, before training. The insets detail the particle distribution in the patterns. (b) As in (a) after training, the probability of finding a pair in mode 0 and 1 is enhanced by more than one order of magnitude. (c) Mean photon number in mode 0 and 1 during the training epochs (green), and expected differential photon number  $\langle(\hat{n}_0 - \hat{n}_1)^2\rangle$  in the two modes, which vanishes after thousands of epochs. The statistical distribution of pairs changes at a constant photon per mode. Data generated by the code in <https://github.com/nonlinearxwaves/BosonSampling>.

Here, we have shown many-body quantum state design and engineering by TensorFlow. We have demonstrated how to enhance multi-particle generation, with many potential applications in quantum technologies.

We acknowledge support from Horizon 2020 Framework Programme QuantERA grant QUOMPLEX, by National Research Council (CNR), Grant 731473.

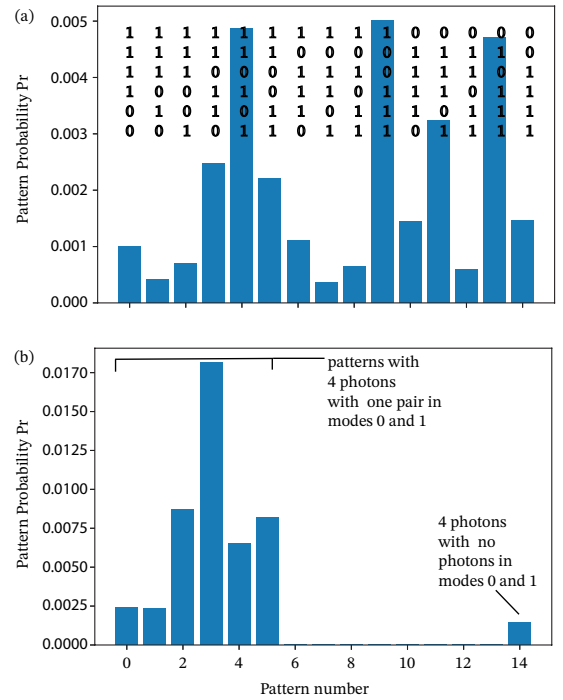


FIG. 4. (a) Probability distribution of patterns with 4 photons ( $n = 6$ ) in the model in Fig. 2c before training. The insets detail the particles in each pattern. (b) As in (a) after training; the probability of patterns with two photons in modes 0 and 1 is maximized. Data generated by the code in <https://github.com/nonlinearxwaves/BosonSampling>.

\* claudio.conti@uniroma1.it

† <https://www.newcomplexlight.org>

- [1] G. Carleo, I. Cirac, K. Cranmer, L. Daudet, M. Schuld, N. Tishby, L. Vogt-Maranto, and L. Zdeborová, Machine learning and the physical sciences, *Rev. Mod. Phys.* **91**, 045002 (2019).
- [2] F. Vicentini, A. Biella, N. Regnault, and C. Ciuti, Variational neural network ansatz for steady states in open quantum systems, *Phys. Rev. Lett.* **122**, 250503 (2019).
- [3] S. Mangini, F. Tacchino, D. Gerace, D. Bajoni, and C. Macchiavello, Quantum computing models for artificial neural networks, (2021), arXiv:2102.03879.
- [4] F. Marquardt, Machine learning and quantum devices, (2021), arXiv:2101.01759.
- [5] A. Lumino, E. Polino, A. S. Rab, G. Milani, N. Spagnolo, N. Wiebe, and F. Sciarrino, Experimental phase estimation enhanced by machine learning, *Phys. Rev. Applied* **10**, 044033 (2018).
- [6] A. Fratallocchi, A. Fleming, C. Conti, and A. D. Falco, Nist-certified secure key generation via deep learning of physical unclonable functions in silica aerogels, *Nanophotonics* **10**, 457 (2021).
- [7] G. Marcucci, D. Pierangeli, P. W. H. Pinkse, M. Malik, and C. Conti, Programming multi-level quantum gates in disordered computing reservoirs via machine learning, *Opt. Express* **28**, 14018 (2020).

- [8] A. A. Melnikov, P. Sekatski, and N. Sangouard, Setting up experimental bell tests with reinforcement learning, *Phys. Rev. Lett.* **125**, 160401 (2020).
- [9] G. Marcucci, D. Pierangeli, and C. Conti, Theory of neuromorphic computing by waves: machine learning by rogue waves, dispersive shocks, and solitons, *Phys. Rev. Lett.* **125**, 093901 (2020).
- [10] T. W. Hughes, I. A. Williamson, M. Minkov, and S. Fan, Wave physics as an analog recurrent neural network, *Sci. Adv.* **5**, eaay6946 (2019).
- [11] D. Ballarini, A. Gianfrate, R. Panico, A. Opala, S. Ghosh, L. Dominici, V. Ardizzone, M. D. Giorgi, G. Lerario, G. Gigli, T. C. H. Liew, M. Matuszewski, and D. Sanvitto, Polaritonic neuromorphic computing outperforms linear classifiers (2019), arXiv:1911.02923.
- [12] J. Nokkala, R. Martínez-Peña, G. L. Giorgi, V. Parigi, M. C. Soriano, and R. Zambrini, Gaussian states provide universal and versatile quantum reservoir computing, (2020), arXiv:2006.04821.
- [13] D. Marković and J. Grollier, Quantum neuromorphic computing, *Appl. Phys. Lett.* **117**, 150501 (2020).
- [14] N. A. Silva, T. D. Ferreira, and A. Guerreiro, Reservoir computing with solitons, *New J. Phys.* **23**, 023013 (2021).
- [15] P. Sgroi, G. M. Palma, and M. Paternostro, Reinforcement learning approach to non-equilibrium quantum thermodynamics, *Phys. Rev. Lett.* **126**, 026601 (2021), arXiv:2004.07770.
- [16] L. Pilozzi, F. A. Farrelly, G. Marcucci, and C. Conti, Topological nanophotonics and artificial neural networks, *Nanotechnology* **32**, 142001 (2021).
- [17] M. Broughton, G. Verdon, T. McCourt, A. J. Martinez, J. H. Yoo, S. V. Isakov, P. Massey, M. Y. Niu, R. Halavati, E. Peters, M. Leib, A. Skolik, M. Streif, D. V. Dollen, J. R. McClean, S. Boixo, D. Bacon, A. K. Ho, H. Neven, and M. Mohseni, Tensorflow quantum: A software framework for quantum machine learning, (2020), arXiv:2003.02989.
- [18] S. M. Barnett and P. M. Radmore, *Methods in Theoretical Quantum Optics* (Oxford University Press, New York, 1997).
- [19] C. S. Hamilton, R. Kruse, L. Sansoni, S. Barkhofen, C. Silberhorn, and I. Jex, Gaussian boson sampling, *Phys. Rev. Lett.* **119**, 170501 (2017).
- [20] N. Quesada, J. M. Arrazola, and N. Killoran, Gaussian boson sampling using threshold detectors, *Phys. Rev. A* **98**, 062322 (2018).
- [21] H.-S. Zhong, H. Wang, Y.-H. Deng, M.-C. Chen, L.-C. Peng, Y.-H. Luo, J. Qin, D. Wu, X. Ding, Y. Hu, P. Hu, X.-Y. Yang, W.-J. Zhang, H. Li, Y. Li, X. Jiang, L. Gan, G. Yang, L. You, Z. Wang, L. Li, N.-L. Liu, C.-Y. Lu, and J.-W. Pan, Quantum computational advantage using photons, *Science* **370**, 1460 (2020).
- [22] M. Tillmann, B. Dakić, R. Heilmann, S. Nolte, A. Szameit, and P. Walther, Experimental boson sampling, *Nat. Photonics* **7**, 540 (2012).
- [23] M. A. Broome, A. Fedrizzi, S. Rahimi-Keshari, J. Dove, S. Aaronson, T. C. Ralph, and A. G. White, Photonic boson sampling in a tunable circuit, *Science* **339**, 794 (2013).
- [24] J. B. Spring, B. J. Metcalf, P. C. Humphreys, W. S. Kolthammer, X.-M. Jin, M. Barbieri, A. Datta, N. Thomas-Peter, N. K. Langford, D. Kundys, J. C. Gates, B. J. Smith, P. G. R. Smith, and I. A. Walmsley, Boson sampling on a photonic chip, *Science* **339**, 798 (2013).
- [25] N. Spagnolo, C. Vitelli, M. Bentivegna, D. J. Brod, A. Crespi, F. Flamini, S. Giacomini, G. Milani, R. Ramponi, P. Mataloni, R. Osellame, E. F. Galvão, and F. Sciarrino, Experimental validation of photonic boson sampling, *Nat. Photonics* **8**, 615 (2014).
- [26] J. Carolan, J. D. A. Meinecke, P. J. Shadbolt, N. J. Russell, N. Ismail, K. Wörhoff, T. Rudolph, M. G. Thompson, J. L. O'Brien, J. C. F. Matthews, and A. Laing, On the experimental verification of quantum complexity in linear optics, *Nat. Photonics* **8**, 621 (2014).
- [27] H. Wang, J. Qin, X. Ding, M.-C. Chen, S. Chen, X. You, Y.-M. He, X. Jiang, L. You, Z. Wang, C. Schneider, J. J. Renema, S. Höfling, C.-Y. Lu, and J.-W. Pan, Boson sampling with 20 input photons and a 60-mode interferometer in a  $10^{14}$ -dimensional hilbert space, *Phys. Rev. Lett.* **123**, 250503 (2019).
- [28] S. Aaronson and A. Arkhipov, The computational complexity of linear optics, *Theory Comput.* **9**, 143 (2013).
- [29] R. Kruse, C. S. Hamilton, L. Sansoni, S. Barkhofen, C. Silberhorn, and I. Jex, A detailed study of gaussian boson sampling, *Phys. Rev. A* **100**, 032326 (2019).
- [30] C. W. Gardiner and P. Zoller, *Quantum Noise*, 3rd ed. (Springer-Verlag, Berlin, 2004).
- [31] X. Wang, T. Hiroshima, A. Tomita, and M. Hayashi, Quantum information with gaussian states, *Phys. Rep.* **448**, 1 (2007).
- [32] A `TensorFlow` implementation in a `Jupyter` notebook is available at <https://github.com/nonlinearxwaves/BosonSampling>.
- [33] J. Johansson, P. Nation, and F. Nori, Qutip 2: A python framework for the dynamics of open quantum systems, *Comput. Phys. Commun.* **184**, 1234 (2013).
- [34] S. Leedumrongwatthanakun, L. Innocenti, H. Defienne, T. Juffmann, A. Ferraro, M. Paternostro, and S. Gigan, Programming linear quantum networks with a multimode fiber, *Nat. Photonics* **14**, 139 (2020), arXiv:1902.10678.
- [35] C. Taballione, T. A. W. Wolterink, J. Lugani, A. Eckstein, B. A. Bell, R. Grootjans, I. Visscher, D. Gekus, C. G. H. Roeloffzen, J. J. Renema, I. A. Walmsley, P. W. H. Pinkse, and K.-J. Boller, Reconfigurable quantum photonic processor based on silicon nitride waveguides, *Opt. Express* **27**, 26842 (2019).
- [36] N. H. Valencia, S. Goel, W. McCutcheon, H. Defienne, and M. Malik, Unscrambling entanglement through a complex medium, *Nat. Phys.* **16**, 1112 (2020).
- [37] N. Quesada and J. M. Arrazola, Exact simulation of gaussian boson sampling in polynomial space and exponential time, *Phys. Rev. Research* **2**, 023005 (2020).
- [38] Y. Li, M. Chen, Y. Chen, H. Lu, L. Gan, C. Lu, J. Pan, H. Fu, and G. Yang, Benchmarking 50-photon gaussian boson sampling on the sunway taihulight, (2020), arXiv:2009.01177.